

# Electron-acoustic-phonon scattering and electron relaxation in two-coupled quantum rings

G. Piacente\* and G. Q. Hai

*Instituto de Física de São Carlos, Universidade de São Paulo,  
13560-970 São Carlos, São Paulo, Brazil*

## Abstract

Electron relaxation, induced by acoustic phonons, is studied for coupled quantum rings in the presence of external fields, both electric and magnetic. We address the problem of a single electron in vertically coupled GaAs quantum rings. Electron-phonon interaction is accounted for both deformation potential and piezoelectric field coupling mechanisms. Depending on the external fields, the ring radii and the separation between the rings, we show that the two different couplings have different weights and importance. Significant oscillations are found in the scattering rates from electron excited states to the ground state, as a function of either the geometry of the system or the external fields.

PACS numbers:

---

\*Electronic address: [gpiacente@ursa.ifsc.usp.br](mailto:gpiacente@ursa.ifsc.usp.br)

## I. INTRODUCTION

Ring geometries have long fascinated physicists for their peculiar features. Recent successful advances in nano-fabrication technology have allowed the realization of self-assembled heterostructured semiconductor rings of nanometer size [1, 2, 3, 4]. These quantum objects, which are nearly disorder free and contain only a few interacting electrons, are attracting a great deal of interest in theoretical and experimental research. Quantum rings (QRs) represent an alternative to quantum dots (QDs) as zero-dimensional structures for practical use as nanodevices. Their not simply-connected geometry provides them with distinctive electronic structures, magnetic field responses and transport properties, which could be of great practical interest.

In the last years much attention has been dedicated to the properties of QDs and coupled quantum dots (CQDs) and their physics is by now well understood. On the other hand, only recently their QR counterparts have started being addressed. A number of experimental and theoretical works have studied laterally-coupled [5], concentrically-coupled [6, 7, 8], vertically-coupled [9, 10, 11, 12] and stacked[13] nanoscopic QRs.

Since the proposal of a qubit based on the electronic states of QDs and CQDs [14, 15], much work has been done in order to understand the carrier-relaxation processes in QDs and CQDs, because a long coherence time is required. The relaxation via phonon emission has received widespread attention. This intrinsic mechanism affects fundamental properties of semiconductor nanostructures and may be the only non-radiative process controlling electron energy losses. Among various aspects of phonon-assisted relaxation, the phonon bottleneck effect, predicted in Ref. [16], was carefully studied. It is the basis of predicted large reductions of electron relaxation rates in QDs when compared to two-dimensional (2D) or one-dimensional (1D) heterostructures. Due to the discrete electron energy spectrum, the interaction with phonons occurs only when the interlevel separation closes to the energy of longitudinal optical (LO) phonons or it is smaller than the bandwidth of acoustic phonons (a few meV). In lateral or vertical QDs, where the energy level separation is small as compared to the optical phonon energies, the electron-acoustic phonon interaction is dominant. In coupled quantum rings (CQRs) the energy separation is of the order of few meV [11], so the relaxation through emission of acoustic phonons is expected to be the most efficient relaxation mechanism.

Electron relaxation in QDs and CQDs due to acoustic phonon scattering has been studied extensively over the past few years [17, 18, 19]. Acoustic phonon induced relaxation has not yet been studied in vertically CQR geometries up to now. In a recent work [20] we investigated the electron relaxation induced by acoustic phonons in a single electron QR in the presence of an external magnetic field. We considered both the deformation potential (DP) and piezoelectric (PZ) acoustic phonon scattering. Motivated by the recent experimental realization of complexes consisting of stacked layers of InGaAs/GaAs QRs [21, 22], here, we face the problem for two vertically coupled quantum rings in the presence of external electric and magnetic fields. Moreover, understanding and controlling the electron relaxation rates is crucial in view of future CQR applications, such as efficient lasers and opto-electronic devices, and in order to achieve high resolution optical spectroscopy, where phonon scattering rates smaller than photon emission and absorption rates are required. Therefore, the knowledge of the physics of electron coupling to acoustic phonon in QRs and CQRs is of great theoretical and practical interest.

The present paper is organized as follows. In Sec. II we summarize the model of CQR we adopt and describe the different electron-phonon coupling mechanisms and the numerical methods we use to calculate the relaxation times. Section III contains the numerical results as well as discussions and comments. Finally, we conclude in Sec. IV.

## II. MODEL AND METHODS

As a prototypical system we consider a GaAs/AlGaAs coupled quantum ring structure, formed by two identical rings coupled along the growth direction, i.e. the  $z$ -direction. The system as a whole has rotational symmetry along  $z$ . We model the two coupled rings with a displaced parabolic confinement in the  $x - y$  plane and a symmetric double-well in the  $z$ -direction:  $V(\mathbf{r}) = \frac{1}{2}m^*\omega_0^2(\mathbf{r}_{\parallel} - r_0)^2 + V_z$ , where  $r_0$  is the ring radius and  $V_z(z) = V_l$  if  $W_b/2 \leq |z| \leq (W_b/2 + W_z)$  and  $V_z(z) = V_h$  otherwise. Here,  $W_z$  is the thickness of the GaAs layers and  $W_b$  is the thickness of the inter-ring layer;  $V_0 \equiv V_h - V_l$  is the conduction band-offset of GaAs/AlGaAs. Furthermore, we consider either a magnetic ( $B$ ) or an electric ( $E_z$ ) field applied in the  $z$ -direction. Since the confinement in the vertical direction is usually much stronger than the lateral one, the in-plane motion and the vertical one can be treated as decoupled, therefore the eigenfunctions are given in the separable form  $\psi_{nmg}(\mathbf{r}) =$

$\phi_{nm}(x, y)\chi_g(z)$ , with the  $n = 0, 1, 2, \dots$ ,  $m = 0, \pm 1, \pm 2, \dots$  (the angular quantum number) and  $g = 0, 1, 2, \dots$ . The functions  $\phi_{nm}(x, y)$  are linear combinations of the Fock-Darwin states for the QD (for details see Refs. [20, 23]), while the functions  $\chi_g(z)$  are the eigenfunctions of the double-well problem. In what follows we will consider only the  $g = 0$  (bonding) and  $g = 1$  (antibonding) states in the vertical direction. Bonding (antibonding) states have even (odd) parity with respect to the reflection about the  $z = 0$  plane.

The electron-phonon scattering rate at zero temperature, where phonon absorption and multi-phonon processes are negligible, can be obtained by the Fermi golden rule, as long as the energy difference between two electron levels is much smaller than the LO-phonon energy [24]. This is the case we study here with  $\hbar\omega_0$  being a few meVs. The scattering rate between the initial state  $\psi_i$  and the final state  $\psi_f$  is given by

$$\tau_{i \rightarrow f}^{-1} = \frac{2\pi}{\hbar} \sum_{\lambda, \mathbf{q}} |M_\lambda(\mathbf{q})|^2 |\langle \psi_f | e^{-i\mathbf{q}\cdot\mathbf{r}} | \psi_i \rangle|^2 \delta(|E_f - E_i| - E_q), \quad (1)$$

where  $M_\lambda(\mathbf{q})$  is the scattering matrix element corresponding to different electron scattering mechanisms  $\lambda$ ,  $\mathbf{q}$  the phonon wave number,  $E_f$  and  $E_i$  the final and initial electron state energies, respectively, and  $E_q$  represents the phonon energy. It is evident from Eq. (1) that the relaxation is mediated by phonons whose energy matches that of the transition between the initial and final electron states.

In a polar semiconductor such as GaAs, electrons couple to all types of phonons, i.e. electrons couple to longitudinal acoustic (LA) phonons through a deformation potential and to longitudinal and transverse acoustic (TA) phonons through piezoelectric interactions [25]. The total scattering matrix element is the sum of all the different contributions.

The electron-LA phonon scattering due to the deformation potential has the form:

$$|M_{\text{LA}}^{\text{DP}}(\mathbf{q})|^2 = \frac{\hbar D^2}{2\rho v_l \Gamma} |\mathbf{q}|, \quad (2)$$

where  $D$ ,  $\rho$ ,  $\Gamma$ , and  $v_l$  are the crystal acoustic deformation potential constant, the density, the volume and the longitudinal sound velocity, respectively. For GaAs (zinc-blende structure) the only nonvanishing independent piezoelectric constant is  $h_{14}$  and the coupling function due to the piezoelectric interaction is given by:

$$|M_{\text{LA}}^{\text{PZ}}(\mathbf{q})|^2 = \frac{32\pi^2 \hbar e^2 h_{14}^2 (3q_x q_y q_z)^2}{\epsilon_0^2 \rho v_l \Gamma |\mathbf{q}|^7}, \quad (3)$$

for the electron - LA phonon scattering and

$$|M_{\text{TA}}^{\text{PZ}}(\mathbf{q})|^2 = \frac{32\pi^2 \hbar e^2 h_{14}^2}{\epsilon_0^2 \rho v_t \Gamma} \left| \frac{q_x^2 q_y^2 + q_y^2 q_z^2 + q_z^2 q_x^2}{|\mathbf{q}|^5} - \frac{(3q_x q_y q_z)^2}{|\mathbf{q}|^7} \right| \quad (4)$$

for the electron - TA-phonon scattering. The transversal sound velocity is written as  $v_t$ . We used linear approximations  $\omega_q^{\text{LA}} = v_l q$  and  $\omega_q^{\text{TA}} = v_t q$  for the LA and TA phonon dispersion, respectively. In our calculation we used GaAs/Al<sub>0.3</sub>Ga<sub>0.7</sub>As material parameters: electron effective mass  $m^* = 0.067$ , band-offset  $V_0 = 240$  meV,  $\rho = 5300$  kg/m<sup>3</sup>,  $D = 8.6$  eV,  $\epsilon = 12.9$ , and  $h_{14} = 1.4 \times 10^9$  V/m. For the sound speeds we used the values  $v_l = 3.7 \times 10^3$  m/s and  $v_t = 3.2 \times 10^3$  m/s [20, 26].

In this work we consider mostly relaxation rates from the first excited to the ground electron state. Since many applications rely on the creation of a two-level system, the relaxation of an electron from the first excited state is often the most relevant transition and, furthermore, it can be monitored, e.g., by means of pump-and-probe techniques [17]. The behavior of transition rates from higher excited states is qualitatively similar, except for the presence of a larger number of decay channels which smears the features of direct scattering between two selected states, as discussed e.g. in Ref. [20].

### III. RESULTS AND DISCUSSION

In order to identify the ground and the first excited electron states, we plot in Fig. 1 the energy levels as a function of the ring radius for different vertical confinements in the absence of external fields. We measure the ring radius in unit  $\alpha_0 = \sqrt{\hbar/m^*\omega_0}$ , which for a lateral confinement  $\hbar\omega_0 = 5$  meV results in a unity length of about 15 nm.

It is interesting to notice the differences between the single QR and CQR cases. The CQR spectrum is much richer than the single QR one due to the presence of antibonding levels which crosses with the bonding ones, a feature which is not present in single QRs. In CQRs even in the absence of magnetic field the ring radius can alter the quantum numbers of excited states. In particular, for  $W_z = 10$  nm the first excited state is a piecewise function of the ring radius, made by the  $(0, 0, 1)$  and  $(0, \pm 1, 0)$  levels. It is also worth noting that a stronger vertical confinement results in a shift to higher energy values for fixed values of the barrier thickness  $W_b$  and ring radius. In the inset of Fig. 1(b), we show the lowest energy levels as a function of  $W_b$  for a fixed value of the ring radius. One can observe that

the energy difference between bonding and antibonding states is a decreasing function with increasing ring separation.

Electron-acoustic phonon relaxation in CQRs is to a large extent determined by the interplay of lateral and vertical confinement strengths relatively to the single rings, inter-ring thickness, and emitted phonon wavelength. Figure 2 shows the scattering rates for the  $(0, 0, 1) \rightarrow (0, 0, 0)$  and  $(0, \pm 1, 1) \rightarrow (0, 0, 0)$  (the inset) transitions as a function of  $W_b$  in the CQRs with  $\hbar\omega_0 = 5$  meV and  $W_z = 10$  nm, for the different scattering mechanisms in the absence of external fields. In particular, we considered values of the  $W_b$  from 2 to 12 nm, accordingly to recent experimental realizations of stacked layers of self-assembled QRs, where the inter-ring thickness were 1.5, 3, 4.5, 6, 10 and 14 nm [21, 22]. The scattering rate oscillates strongly for the  $(0, 0, 1) \rightarrow (0, 0, 0)$  transition as a function of  $W_b$ , on the other hand such oscillations are not found in the  $(0, \pm 1, 0) \rightarrow (0, 0, 0)$  transition. The reason for these oscillations is that the electron wave function along the  $z$ -direction can be in-phase or in anti-phase with the phonon wave, in particular, there are maxima when the electron wave function is in-phase with the phonon wave and minima when the electron wave function is in anti-phase with the phonon wave. The tunneling energy in CQRs depends on the barrier thickness  $W_b$  between the two rings: tunneling between the rings affects strongly the electron-phonon interaction because the electron wave function spreads in the two rings leading to different phonon wavelengths matching the electron-phonon interference. For the sake of clarity, the energy, and thus the wavelength of the emitted phonon, of the  $(0, 0, 1) \rightarrow (0, 0, 0)$  transition from an antibonding to a bonding state is exclusively related to the inter-ring thickness, while the energy of the  $(0, \pm 1, 0) \rightarrow (0, 0, 0)$  transition from a bonding to another bonding state is related to the lateral confinement only. Therefore, if we fix the lateral confinement and change the inter-ring thickness, we get strong oscillations in the scattering rate for the  $(0, 0, 1) \rightarrow (0, 0, 0)$  transition. On the other hand, if we fix the inter-ring thickness and change only the lateral confinement, we get strong oscillations in the scattering rate for the  $(0, \pm 1, 0) \rightarrow (0, 0, 0)$  transition (see Fig. 3).

From Fig. 2 one can see that for small ring separations in the  $(0, 0, 1) \rightarrow (0, 0, 0)$  transition the LA-DP scattering is much more efficient than the LA-PZ and TA-PZ ones, while for larger values of the barrier thickness the LA-PZ and TA-PZ couplings start to dominate over the LA-DP one. However, for the  $(0, \pm 1, 0) \rightarrow (0, 0, 0)$  transition the LA-DP scattering is always larger than the other ones. Furthermore, the TA-PZ scattering is generally larger

than the LA-PZ one, except for large  $W_b$ .

In what follows we concentrate on geometries characterized by  $W_z = 10$  nm and  $W_b = 5$  nm. Figure 3 illustrates the scattering rate for a CQR system as a function of the lateral confinement energy  $\hbar\omega_0$ . For most lateral confinements and for  $r_0 = 2\alpha_0$ , DP coupling gives the largest contribution and the PZ coupling is negligible. However, for very weak confinements in the  $(0, \pm 1, 0) \rightarrow (0, 0, 0)$  transition (see the inset), the PZ coupling prevails. This is a result in agreement with recent findings in CQDs [19]. As already mentioned, strong oscillations in the scattering rate are present in the  $(0, \pm 1, 0) \rightarrow (0, 0, 0)$  transition, but not in the  $(0, 0, 1) \rightarrow (0, 0, 0)$  transition, just the opposite with respect to the case of the dependence of barrier thickness. In the presence of strong oscillations the scattering rate is suppressed by orders of magnitude. This phenomenon, already observed in QDs and CQDs [19] and in QRs [20], has been proposed as a possible way to preserve the quantum coherence in view of the implementation of quantum computing devices based on semiconductor nanostructures [27].

Although the shape of PZ scattering rate is different from the DP one as a function of  $\hbar\omega_0$ , the limiting behavior is similar: they tend to zero at very weak confinement potentials because of the vanishing phonon density. Moreover, we observe again that the PZ contribution coming from the TA phonons is larger than that of the LA phonons. This holds for almost all the calculations throughout this paper.

In Fig. 4 we study the electron relaxation in CQRs in the case  $B = 0$  as a function of the ring radius  $r_0$  at  $B = 0$ . In particular, we deal with the CQRs with  $\hbar\omega_0 = 5$  meV and  $W_z = 10$  nm. This choice is justified by the fact that in experimental realization of QRs the radius is found to be  $r_0 \sim 15 \div 60$  nm and the ring thickness is found to be  $W_z \sim 10$  nm [2, 4, 28]. In the rest of the paper we will consider rings with such values of lateral and vertical confinements. The total relaxation time for the transition from the first excited to the ground state is shown in the picture, while the contributions arising from the different scattering mechanisms are shown in the inset. All the curves present a discontinuity corresponding to the  $(0, 0, 1)$  and  $(0, \pm 1, 0)$  crossings. The total relaxation time is of the order of fractions of nanoseconds and presents a modulation with varying radius. More interesting information comes from observing the different contributions from DP and PZ couplings: for small ring radius the LA-DP scattering is order of magnitude larger than the LA-PZ and TA-PZ scatterings, in agreement with the case of CQDs. In this

case the PZ coupling can be disregarded: this is the reason why DP coupling is often the only source of decoherence considered in the literature. On the other hand, PZ scattering is much larger than DP for large  $r_0$ . There is a clear crossover from which the PZ coupling starts to dominate over the DP one ( $r_0 > 3\alpha_0$ ). This findings are similar to the ones in Ref. [20] for single QRs, so we can conclude that the efficacy of the PZ scattering is intimately related to the ring topology and, hence, in QRs and CQRs PZ effects are always important and cannot be disregarded.

When a vertical magnetic field is present new effects appear. First of all, as one can see in Fig. 5(a) and (b) the typical level crossings of multiple connected geometries appear in the energy spectra. The ground state, for instance, changes from the state with  $m = 0$  to the ones with  $m = -1, -2, -3, \dots$ . It is worth stressing that this feature is not present in QDs and CQDs, where no level crossings for the ground state occur, even in the presence of strong magnetic fields, and the low-lying levels converge to the first Landau levels without crossings. Actually, identifying the crossing points in the energy spectra gives straightforward information about the specific ring topology [10, 29]. In the presence of magnetic field the number of crossing points is strongly increasing with increasing  $r_0$ , as is evident in comparing Figs. 5(a) and 5(b). Moreover, the low-lying levels are bonding states when a vertical magnetic field is applied.

For fixed ring radii  $r_0 = 2\alpha_0$  and  $r_0 = 3\alpha_0$ , we calculate the scattering rates among the first excited state to the ground state as a function of magnetic field. The results are shown in Figs. 6(a) and 7(a), respectively. The contributions of the DP and PZ phonons to the scattering rates are given separately in Figs. 6(b) and 7(b). The first notable features is that in both cases the total relaxation rate shows oscillations with striking dips corresponding to the level crossing points. This property is related to the fact that the scattering matrix elements  $|\langle \phi_{n',m'} | M_\lambda^2(\vec{\mathbf{q}}) | \phi_{n,m} \rangle|^2$  vanish in correspondence of a crossing point, where  $q_0 = 0$ . The number of dips increases with increasing radius, because the number of level crossings is larger for larger radius. Furthermore, the PZ and DP phonon scattering rates have approximatively the same magnitude and they both contribute to the total scattering rate. This is very different from the CQD case. Actually, in CQDs in the presence of vertical magnetic fields up to 5 Tesla the PZ rates are always orders of magnitude smaller than the DP ones [19]. Once more, this confirms and stresses that the scattering mechanism is significantly different between rings and dots and that such a difference is amplified when a



magnetic field is applied. In order to describe properly the phonon scattering processes in the CQRs in magnetic fields, inclusion of the PZ interaction is, therefore, fundamental.

Finally, we study the effect of an external electric field along the vertical direction. In Fig. 8 we depict the  $E_z$ -dependent scattering rate in CQRs with different ring radii in the absence of magnetic field. Applying a vertical electric field is an efficient way to tune the tunneling, therefore it influences the transition between states with different parities. In fact, we find strong oscillations of the DP and PZ scattering rates for the  $(0, 0, 1) \rightarrow (0, 0, 0)$  transition, while the scattering rates for the  $(0, \pm 1, 0) \rightarrow (0, 0, 0)$  transition are almost constant. Interestingly, the PZ scattering rate decays much faster than that of the DP in the  $(0, 0, 1) \rightarrow (0, 0, 0)$  transition. Although PZ and DP scatterings have about the same magnitude in the absence of external fields for relatively small ring radii, the application of an electric field soon turns DP into the dominant relaxation mechanism and drastically reduces the PZ scattering, as one can see in Figs. 8(a) and 8(b). For relatively large ring radii [see Figs. 8(c) and 8(d)] the situation is different and more complex. As a matter of fact for the  $(0, \pm 1, 0) \rightarrow (0, 0, 0)$  transition the PZ scattering is larger than the DP one, while for  $(0, 0, 1) \rightarrow (0, 0, 0)$  transition the DP relaxation rate is order of magnitude larger than the the DP one.

#### IV. CONCLUSIONS

We studied the acoustic phonon induced electron relaxation in vertically coupled GaAs quantum rings, which is of fundamental importance for applications of quantum rings as quantum gates and nanodevices. We investigated how ring geometry, inter-ring tunneling, and external fields affect the electron-phonon scattering and the relaxation from the first excited state to the ground state. Our calculations show that the electron-phonon scattering strongly depends on the ring size, separation between the two QRs, and on external fields. We took into account both deformation potential and piezoelectric field couplings and demonstrated that they both give important contributions to the electron relaxation. Piezoelectric interactions, often neglected in the literature in the studies of relaxation in quantum dots and coupled quantum dots, represent the major source of scattering in the presence of external magnetic field and for large ring radius and/or large ring separation, while for small ring radius and zero external field deformation potential couplings prevail.

Furthermore, we have shown that significant oscillations in the scattering rates from electron excited states to the ground state are present and depend on either the geometry of the structure or the external fields.

## V. ACKNOWLEDGMENTS

This work was supported by FAPESP and CNPq, Brazil

---

- [1] J. M. Garcia, G. Medeiros-Ribeiro, K. Schmidt, T. Ngo, J. L. Feng, A. Lorke, J. P. Kotthaus, and P. M. Petroff, *Appl. Phys. Lett.* **71**, 2014 (1997).
- [2] A. Lorke, R. J. Luyken, A. O. Govorov, J. P. Kotthaus, J. M. Garcia, and P. M. Petroff, *Phys. Rev. Lett.* **84**, 2223 (2000).
- [3] D. Maily, C. Chapelier, and A. Benoit, *Phys. Rev. Lett.* **70**, 2020 (1993).
- [4] T. Mano, T. Kuroda, S. Sanguinetti, T. Ochiai, T. Tateno, J. Kim, T. Noda, M. Kawabe, K. Sakoda, G. Kido, and N. Koguchi, *Nano Lett.* **5**, 425 (2005).
- [5] J. Planelles, F. Rajadell, J. I. Climente, M. Royo, and J. L. Movilla, *J. Phys.: Condens. Matter* **17**, 1573 (2005).
- [6] T. Kuroda, T. Mano, T. Ochiai, S. Sanguinetti, K. Sakoda, G. Kido, and N. Koguchi, *Phys. Rev. B* **72**, 205301 (2005).
- [7] B. Szafran and F. M. Peeters, *Phys. Rev. B* **72** 155316 (2005).
- [8] J. Planelles and J. I. Climente, *Eur. Phys. J. B* **48**, 65 (2005).
- [9] D. Granados, J. M. Garcia, T. Ben, and S. I. Molina, *Appl. Phys. Lett.* **86**, 071918 (2005).
- [10] J. I. Climente and J. Planelles, *Phys. Rev. B* **72**, 155322 (2005).
- [11] F. Malet, M. Barranco, E. Lipparini, R. Mayol, M. Pi, J. I. Climente, and J. Planelles, *Phys. Rev. B* **73**, 245324 (2006).
- [12] L. K. Castelano, G. Q. Hai, B. Partoens, and F. M. Peeters, *Phys. Rev. B* **74**, 045313 (2006).
- [13] K. H. Ahn and P. Fulde, *Phys. Rev. B* **62**, R4813 (2000).
- [14] M. Bayer, P. Hawrylak, K. Hinzer, S. Fafard, M. Korkusinski, Z. R. Wasilewski, O. Stern, and A. Forchel, *Science* **291**, 451 (2001).
- [15] G. Burkard, G. Seelig, and D. Loss, *Phys. Rev. B* **62**, 2581 (2000).

- [16] U. Bockelmann and G. Bastard, Phys. Rev. B **42**, 8947 (1990).
- [17] T. Fujisawa, D. G. Austing, Y. Tokura, Y. Hirayama, and S. Tarucha, Nature (London) **419**, 278 (2002).
- [18] G. Ortner, R. Oulton, H. Kurtze, M. Schwab, D. R. Yakovlev, M. Bayer, S. Fafard, Z. Wasilewski, and P. Hawrylak, Phys. Rev. B **72**, 165353 (2005).
- [19] J. I. Climente, A. Bertoni, G. Goldoni, and E. Molinari, Phys. Rev. B **74**, 035313 (2006).
- [20] G. Piacente and G. Q. Hai, Phys. Rev. B **75**, 125324 (2007).
- [21] D. Granados, J. M. Garca, T. Ben, and S. I. Molina, Appl. Phys. Lett. **86**, 071918 (2005).
- [22] F. Suárez, D. Granados, M. L. Dotor and J. M. Garca, Nanotechnology **15**, S126 (2004).
- [23] J. Simonin, C. R. Proetto, Z. Bartevisa, and G. Fuster, Phys. Rev. B **702**, 205305 (2004).
- [24] G. Q. Hai and S. S. Oliveira, Appl. Phys. Lett. **88**, 196101 (2006).
- [25] G. D. Mahan, *Many-Particle Physics* (Plenum Press, New York, 1990).
- [26] J. S. Blakemore, J. Appl. Phys. **53**, R123 (1982).
- [27] P. Zanardi and F. Rossi, Phys. Rev. Lett. **21**, 4752 (1998).
- [28] A. Emperador, M. Pi, M. Barranco, and A. Lorke, Phys. Rev. B **62**, 4573 (2000).
- [29] A. Fuhrer, S. Lüscher, T. Ihn, T. Heinzel, K. Ensslin, W. Wegschel, and M. Bichler, Nature (London) **413**, 822 (2001).

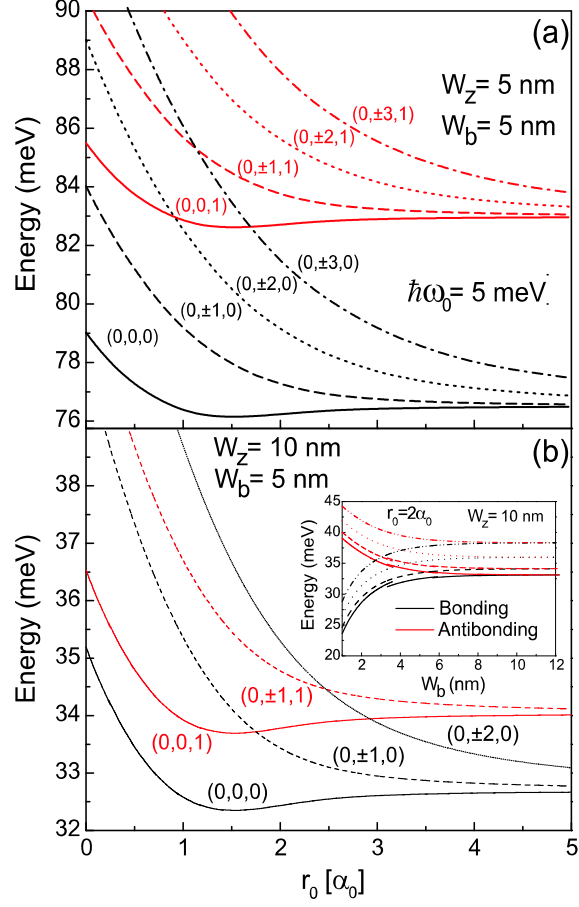


FIG. 1: (Color online) The energy spectrum for  $B = 0$  as a function of the ring radius at fixed lateral confinement  $\hbar\omega_0 = 5$  meV: (a) for  $W_b = 5$  nm and  $W_z = 5$  nm; (b)  $W_b = 5$  nm and  $W_z = 10$  nm. In (b) the inset shows the lowest bonding and antibonding levels as a function of the ring separation  $W_b$  for  $r_0 = 2\alpha_0$ .

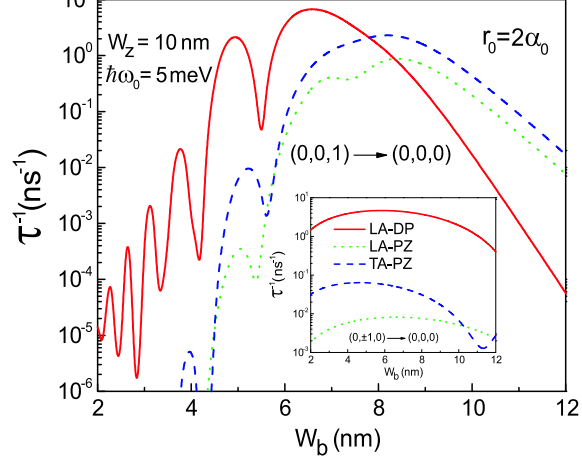


FIG. 2: (Color online) The LA-DP, LA-PZ and TA-PZ scattering rates for the  $(0, 0, 1) \rightarrow (0, 0, 0)$  transition as a function of the barrier thickness  $W_b$ . The inset shows the scattering rates for the  $(0, \pm 1, 0) \rightarrow (0, 0, 0)$  transition.

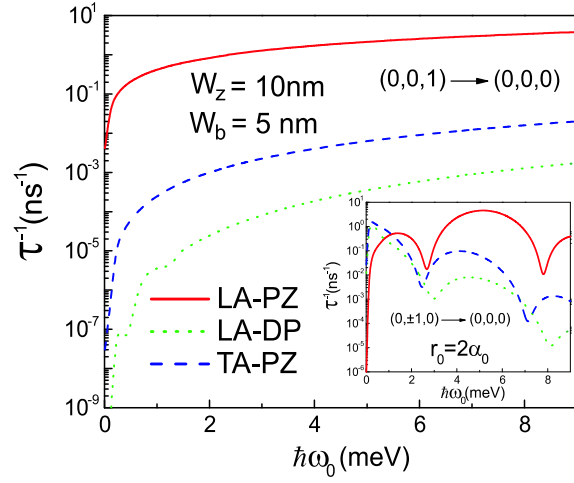


FIG. 3: (Color online) The LA-DP, LA-PZ and TA-PZ scattering rates for the  $(0, 0, 1) \rightarrow (0, 0, 0)$  transition as a function of the lateral confinement  $\hbar\omega_0$ . The inset shows the scattering rates for the  $(0, \pm 1, 0) \rightarrow (0, 0, 0)$  transition.

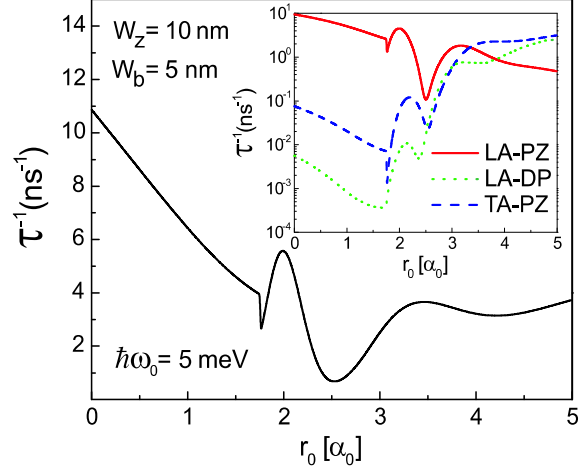


FIG. 4: (Color online) (a) The total relaxation rate for the transition from the first excited state to the ground state as a function of the ring radius; (b) the LA-DP, LA-PZ and TA-PZ contributions.

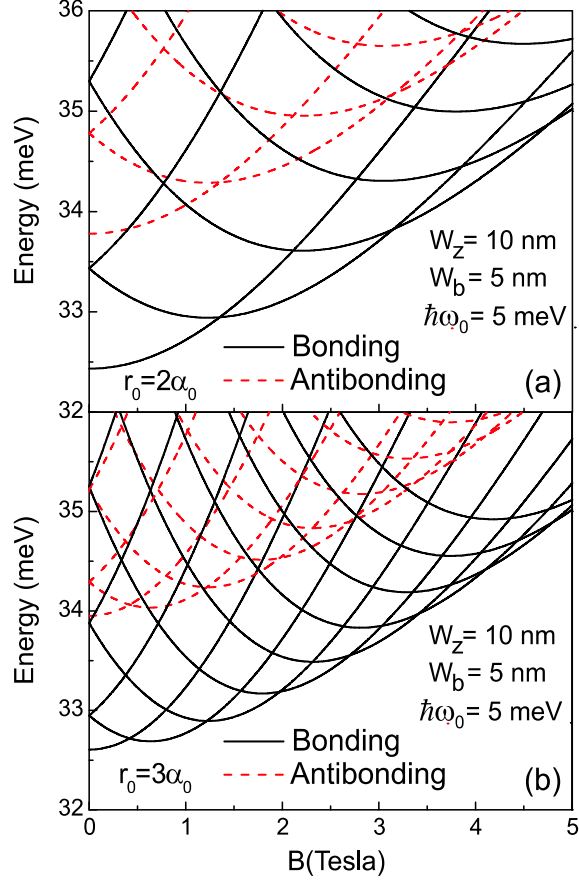


FIG. 5: (Color online) The energy spectrum as a function of the external magnetic field: (a) for  $r_0 = 2\alpha_0$  and (b)  $r_0 = 3\alpha_0$ . The solid lines represent bonding states, while the dashed lines are relative to antibonding states.

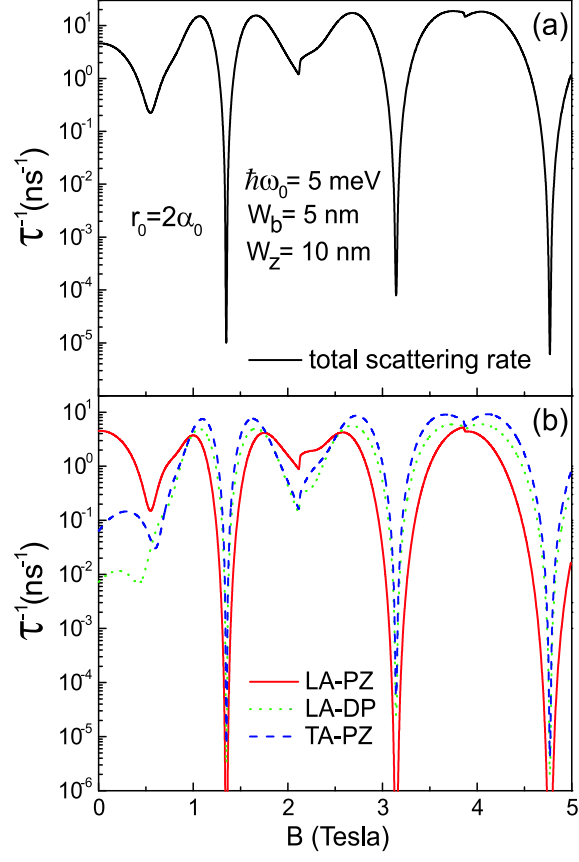


FIG. 6: (Color online) (a) The total relaxation rate from the first excited state to the ground state as a function of the magnetic field for a ring of radius  $r_0 = 2\alpha_0$ ; (b) the LA-DP, LA-PZ and TA-PZ contributions.



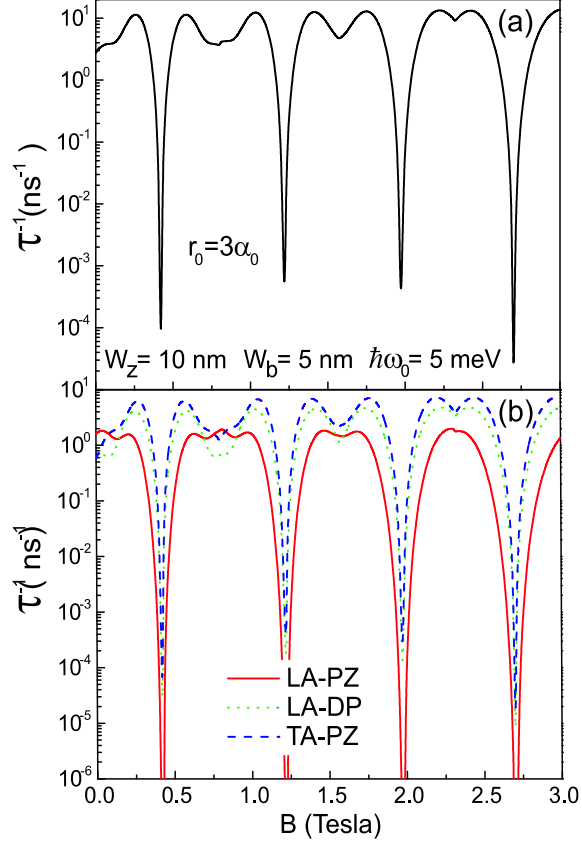


FIG. 7: (Color online) The same as Fig. 6, but with  $r_0 = 3\alpha_0$ .

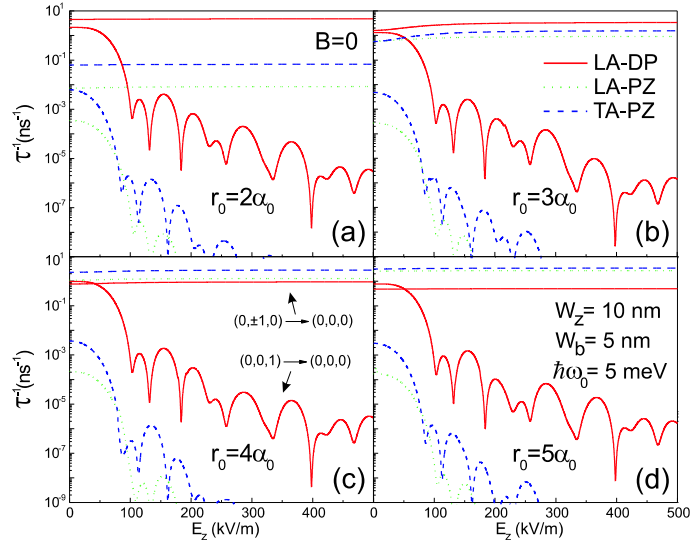


FIG. 8: (Color online) The different scattering mechanisms as a function of vertical electric field for the  $(0, 0, 1) \rightarrow (0, 0, 0)$  and  $(0, \pm 1, 0) \rightarrow (0, 0, 0)$  transitions for different ring radii.